Development of interaction diagrams for RC sections confined with CFRP composites

P. Christou, A. Michael & Z. Neofytou
Department of Civil Engineering, Frederick University, Cyprus

Abstract

The interaction diagram is a surface which defines the maximum capacity of compression members that are subjected to axial force and bending moments. As a result, these diagrams provide the engineers with an additional tool for the design of such members. When the compression members are confined with FRP their capacity increases, however in many cases the increase in capacity is normally neglected which sometimes can lead to very conservative designs. This work includes the development of interaction diagrams for circular compression members confined with CFRP using the fiber model. The longitudinal reinforcement is considered to be symmetric whereas the confinement can vary. The method presented herein defines the location of the neutral axis and based on that calculates the axial force and bending moment. A comparison of the unconfined to the confined section shows a considerable difference in the interaction diagram plot in the compression controlled region.
Keywords: interaction diagrams, confinement, section equilibrium, RC section strength.

1 Introduction

The analysis of concrete columns using an analytical solution is not trivial. As a result the analysis of columns is basically reduced to the development of the interaction diagram and the plot of the load condition in order to define failure or not for the section. Normally the confinement for compression reinforced concrete sections is provided either by ties or spirals. However, other methods and materials are used in the later years which can provide increased confinement and thus satisfy the requirement for increased ductility. The column wrapping with CFRP composites is a popular alternative for improving the

WIT Transactions on Modelling and Simulation, Vol 51, © 2011 WIT Press
www.witpress.com, ISSN 1743-355X (on-line)
doi:10.2495/CMEM110341

ductility and thus the seismic resistance of columns. Fiber fabrics and prefabricated FRP composite jackets or tubes cover the entire area of the concrete element and therefore cannot be embedded in concrete. Another technique is the use of a CFRP composite grid (Michael *et al.* [1]). The carbon grid has approximately 69% open surface area allowing the grid to be embedded in the concrete. Light grids are easily formed into a round shape and can provide more effective confinement than wraps that are forced to follow the column cross-section, which might be square or rectangular.

The work presented herein refers to a numerical procedure for the development of interaction diagrams that are confined with CFRP and provide a comparison with similar sections without confinement.

1.1 Approximate analyses for columns

A search in the literature reveals a number of numerical approximations for the development of such diagrams. In the three dimensional case these methods rely on using single axis bending response in the two principal directions for the approximation of the biaxial bending. Some of these methods are:

- The Bressler load contour method [2]
- The Bressler reciprocal load method [2]
- The PCA load contour method [2]
- The Weber design charts [3]

1.2 Confined concrete

Confinement can improve both the compressive strength and ductility of concrete. Steel has typically been used to confine the concrete in reinforced concrete columns. Steel can be internal reinforcement, usually used as a spiral or ties, or it can be external such a steel jacket that is bonded to the outside face of the column. When fiber reinforced polymer (FRP) materials became widely available in the civil sector they started replacing steel as external confinement reinforcement. One of the primary applications of FRP materials is retrofit of concrete elements, primarily columns, to improve their ductility. This is done mainly in seismic regions where concrete structures experience large deformations. Column wrapping improves the strength and ductility of the concrete and improves its performance under earthquake loads. Xiao and Wu [4, 5] wrapped concrete cylinders using various materials and methods. Some were wrapped with carbon fiber fabrics, while others were wrapped with glass fiber fabrics. They also wrapped cylinders using a machine that tightly wound carbon fibers around the cylinders. The results showed a significant improvement both in strength and ductility. Lam and Teng [6], Li *et al*. [7] and Harries and Kharel [8] wrapped cylinders with carbon fabrics with similar results as Xiao and Wu [4]. Li and Hadi [9] and Campione and Miraglia [10] tested round concrete columns wrapped with either glass or carbon fiber fabric sheets in a polymer matrix. In doing so they improved the ductility of the columns. Campione and Miraglia [10] also wrapped, in the same manner, square columns and square columns with round corners with the same results. It was found that the round

shape is the most effective shape for confinement while the square with sharp corners the least effective of the three. Teng *et al*. [11] wrapped bridge columns in the field using FRP wraps. Laboratory specimens were also tested with the columns exhibiting a ductile behavior. Shahawy *et al*. [12] tested standard concrete cylinders wrapped with carbon fiber fabrics in an epoxy matrix. The results varied depending on the number of carbon layers applied. For an unconfined concrete strength of 41.4 MPa the confined strength of cylinders was increased to 70 MPa for the 1-layer wrap and 110 MPa for the 4-layer wrap. The ultimate strain for the 1-layer wrap was 0.007 and for the 4-layer wrap 0.016. Prefabricated FRP tubes can be filled with concrete and serve at the same time as formwork, flexural reinforcement and confinement reinforcement. Davol *et al*. [13] tested prefabricated round shells filled with concrete in flexure with satisfactory results. The concrete filled FRP shells exhibited a ductile behavior. Michael *et al*. [1] used a light CFRP composite grid to confine concrete. Through a series of cylinder tests they found that the grid provides light confinement to concrete. The crushing strain of confined concrete was twice as high compared to the unconfined concrete tested. Michael *et al*. [1] used the CFRP composite grid in a series of flexural members and had improvements in the member ductility of more than 30% with minimal confinement reinforcement.

2 Interaction diagrams

The interaction diagram (fig. 1) is a graphical representation of the ultimate capacity of a column subjected to axial load (Pn) and uniaxial bending (Mn). The

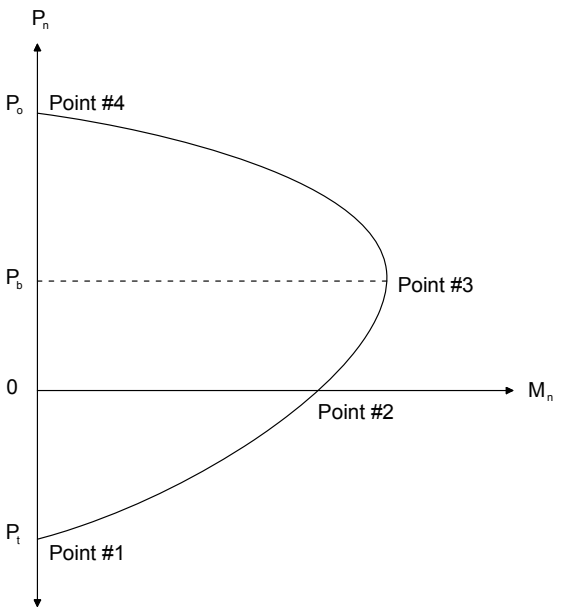

Figure 1: Interaction diagram.

interaction diagram depends on the concrete cross sectional area, the material properties (stress and strain) and also the amount and distribution of reinforcement. Therefore, each concrete section with a specific reinforcement distribution is characterized by a unique interaction diagram representing failure as the crushing of concrete at the maximum compressive strain. After the determination of design loads (P, M) three possible load conditions plotted as points can be defined once the interaction diagram for a section is obtained:

- The load condition coincides with the interaction diagram curve: represents the limit state.
- The load condition falls inside the interaction diagram curve: causes no failure in the section.
- The load condition falls outside the interaction diagram curve: causes failure in the section.

The interaction diagrams can also be extended to three dimensional surfaces to account for biaxial bending. The principle regarding the load conditions remains the same.

3 Requirements for the development of interaction diagrams

The following conditions, assumptions and limitations, the definition of the stress vs strain relations of the material as well as the definition of the plastic centroid of the section are required for the development of interaction diagrams.

3.1 Conditions

The following conditions must be satisfied in the development of the interaction diagram.

- Force equilibrium
- Strain Compatibility
- Stress vs Strain relationships

3.2 Assumptions and limitations

The following assumptions and limitations are applied.

- Plane sections remain plane
- The strain in the reinforcement is the same as that of the adjacent concrete interface
- The tensile strength of concrete is neglected
- Failure occurs in the concrete at maximum compressive strain

3.3 Stress vs strain properties

In this section the stress strain relationships for the materials are presented. The sections that are examined refer to reinforced column sections without any confinement and then compared to similar sections that are confined with CFRP.

3.3.1 Concrete

The stress – strain relation in the concrete that is used in this work is represented by the parabola defined by Hognestad as this is defined in the literature [14]. The tensile part of the graph is neglected. In order to define the curve it is required to have the concrete strength (f'_c), the strain at peak stress, ε_o, and the concrete modulus of elasticity (E_c).

3.3.2 Steel

The stress – strain relation is assumed to be elastic-plastic and it is the same in tension and compression [14]. In order to define this curve it is required to define the steel yield stress (f_y) and the modulus of elasticity of steel (E_s).

3.3.3 Experimental confinement model

Most models for concrete confined with CFRP reinforcement are based on the fact that in most cases even one layer of carbon fabric or a carbon jacket will provide enough reinforcement to have highly confined concrete. Therefore, the confinement effectiveness is high leading to a failure of the CFRP jacket or encasement at the peak axial stress. When the CFRP grid is used as confinement reinforcement the confining pressure and confinement effectiveness is low and therefore models developed using data from relatively high confined concrete may not be adequate. To model the behavior of CFRP grid confined concrete existing models were used. Existing models are based on a constant thickness of the FRP material that covers all of the surface area of the confined concrete core. Michael *et al.* [1] used the modified Hognestad stress–strain curve to model the behavior of CFRP grid confined concrete as shown in fig. 2 [1]. In fig 2 ε_c is the

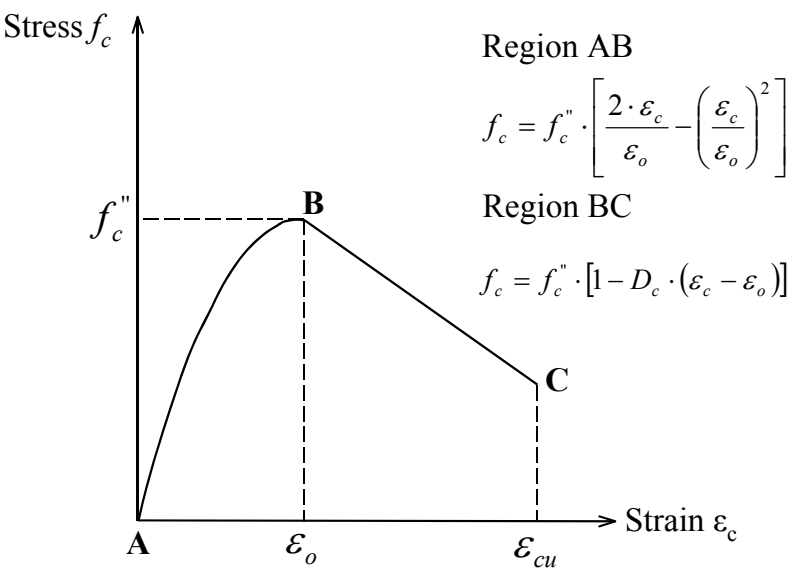

Figure 2: Modified Hognestad parabola used for the modeling of confined concrete [1].

concrete strain, ε_o is the strain at peak stress of unconfined concrete and ε_{cu} is the ultimate strain. The modified Hognestad parabola consists of two regions. In region AB ($\varepsilon_c < \varepsilon_o$) the Hognestad parabola is used and in region BC ($\varepsilon_o < \varepsilon_c < \varepsilon_{cu}$) a linearly descending curve. The equation for region BC is based on the deterioration constant (D_c) that controls the slope of the line. The equations for the two regions were modified to model the behavior of CFRP grid concrete. The material properties of the CFRP grid strands were used in the process of constructing the stress-strain curve of the CFRP grid confined concrete. The average strength of the control cylinders tested in deflection control model was taken as the strength of unconfined concrete (f'_c). The ultimate concrete strain ε_{cu} was assumed to be 0.00725 mm/mm. The deterioration constant was taken equal to 130 to match post peak experimental data. All three curves are depicted in fig. 3. The modified Hognestad matches well with the experimental curve.

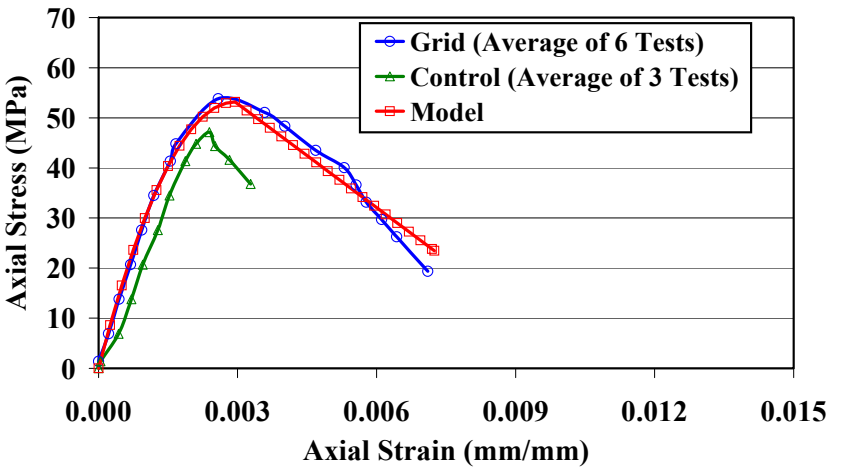

Figure 3: Concrete modelling as obtained by experimental data [1].

3.4 Plastic centroid

Reference must be made as to the point about which the moments are calculated. We refer to this point as the plastic centroid and it is the point of action of the axial load when there is a uniform maximum compressive strain. This assures that the moment capacity of the section is zero at maximum axial load capacity.

4 Development of the interaction diagram

The development of the interaction diagram is based on the calculation of a series of points representing failure in the concrete subjected to maximum compressive strain and a specified strain in the extreme steel fiber. A number of points, axial force vs bending moment (Pn, Mn) are calculated in order to define

the failure curve of the section. The calculation of individual points ensures equilibrium of the section and it includes:

- The definition of the neutral axis location
- The calculation of the plastic centroid
- The definition of the strain plane over the entire section
- The calculation of strains using compatibility and the corresponding stresses based on the stress vs strain relation
- The integration of stresses over the section to calculate the axial force and the bending moment

4.1 Neutral axis location

The neutral axis location is calculated using the values of the maximum compressive strain in the concrete, ε_{cu}, and a variable value for the strain in the extreme reinforcing steel fiber, ε_{st}. Each combination of strains (ε_{cu}, ε_{st}) will define a strain distribution over the section at failure and thus a point on the interaction diagram (axial load vs bending moment). The calculation of the neutral axis in a circular section can take advantage of the symmetry of the section. One point on the section (P_1) is assigned the maximum compressive strength and it is considered the extreme concrete compression fiber. The extreme steel fiber is located at the steel bar which is located at the maximum distance from the extreme compression fiber. Having the location of the two extreme fibers and the values of the corresponding strains the neutral axis can be defined as shown in fig. 4.

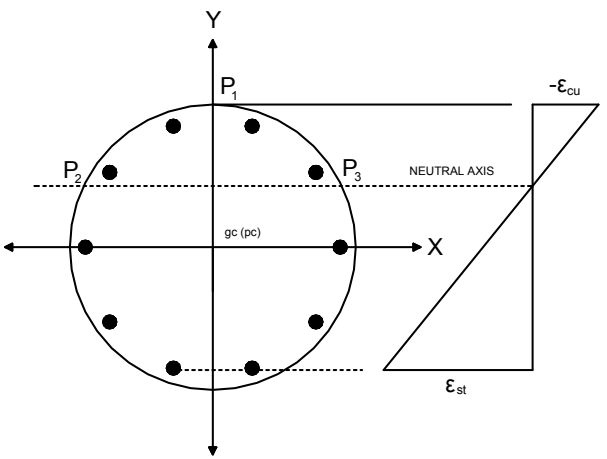

Figure 4: Rectangular cross sectional data.

4.2 Plastic centroid location

For symmetrical sections both in concrete geometry as well as the reinforcement distribution the plastic centroid (pc) coincides with the geometric centroid (gc).

When this is not the case then the location of the plastic centroid has to be calculated accounting for the concrete geometry as well as the area and location of each reinforcing bar.

4.3 Strain plane and calculation of strains

When the neutral axis is defined the distribution of the strain over the whole section can be defined with the calculation of a strain plane. The strain plane is defined using two points on the line of the neutral axis (P_2, P_3) and the point at the extreme compression fiber (P_1) as shown on fig. 4.

Using the strain plane equation a strain value for any point on the section can be defined. Based on the strain and the stress vs strain relation of the material the stress at each point can be obtained using eqn (1).

$$dF_i = \sigma_i dA_i \tag{1}$$

4.4 Integration of stresses to calculate axial load and bending moment

The axial load (P_n) and bending moment (M_n) can be calculated by the integration of stresses over the section. This can be done using eqn (2) and eqn (3):

$$P = \iint_A dF_i = \iint_A \sigma_i dA \tag{2}$$

$$M = \iint_A dF_i \; x = \iint_A \sigma_i \; x \; dA \tag{3}$$

4.5 Numerical procedure for the generation of the interaction diagram

The direct integration for the calculation of the axial load as well as the moment is not trivial. For this reason a numerical procedure (and accompanying software) was developed and used in this work for the generation of the interaction diagrams. The range of the axial loads spans from the maximum compressive axial load to the axial load of pure tension. In order to numerically generate the diagram four points are identified on it (fig. 1).

- Point #1: Fracture failure point (pure tension)
- Point #2: Zero axial load point
- Point #3: Balanced point
- Point #4: Maximum compressive axial load point (pure compression)

These points are calculated independently and they define three (3) sub regions on the diagram. For each Point the important element to be known is the value of the net tensile strain at the extreme tension reinforcement fiber. The strains at Point #1, Point #3 and Point #4 are known directly from material properties. The other one has to be calculated. The strain at Point#2 represents the point with zero axial load. However, the strain in the extreme reinforcement bar is not known. As a result an iteration convergence procedure (secant method)

is used to calculate the strain in the extreme steel fiber when the axial load equals to zero. Once the strains for the boundary points of the sub regions are defined, the diagram can be generated by assigning different values of strains for the extreme steel fiber in each sub region and thus calculating intermediate points within the sub regions on the interaction diagram. Fig. 5 shows the flowchart of the numerical procedure.

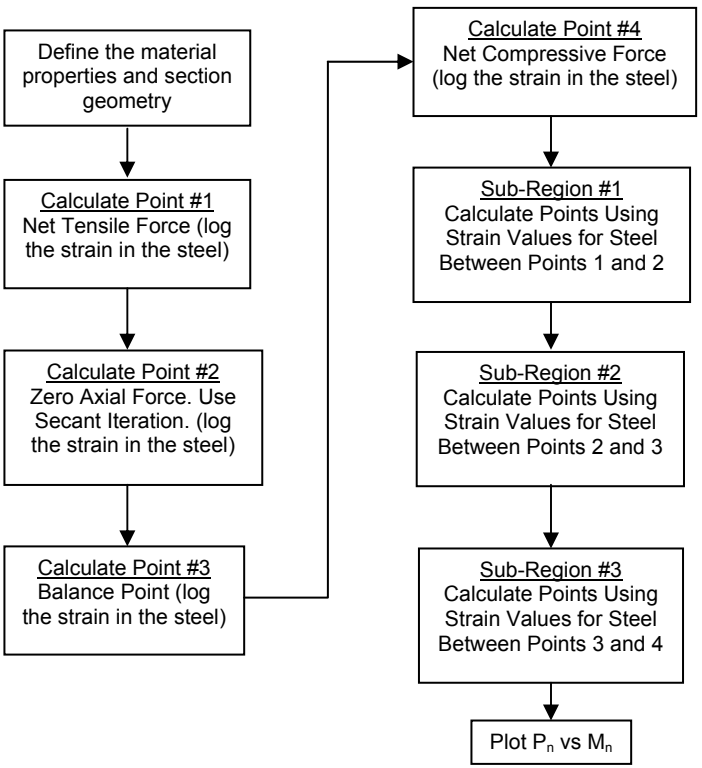

Figure 5: Flowchart describing the numerical procedure.

5 Example

The presented procedure has been used for the development of the interaction diagram of different sections. Fig. 6 shows the interaction diagram of the same section with three different levels of concrete strength. The inner line shows the unconfined section whereas the intermediate line shows the section with confinement strength as described in section 3.3.3 (Experimental results). The outer line shows the section using the same model for confinement as that of section 3.3.3 but with a different value of the maximum compressive strength. Particularly the data is shown below:

5.1 Section data

Section Radius	25 cm
Reinforcement	10 bars (dia=16 mm) distributed uniformly
ε_{cu} (Unconfined)	0.003 mm/mm
ε_{cu} (Confined)	0.00725 mm/mm
f'_c (Unconfined)	40 MPa
f'_c (Confined – 1)	54 MPa
f'_c (Confined - 2):	60 MPa
D_c (Deterioration Constant)	130

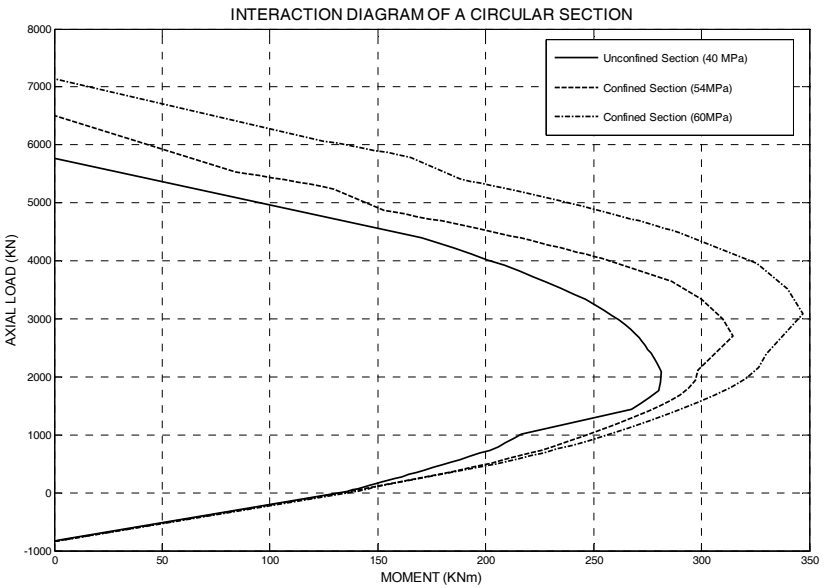

Figure 6: Section comparison with variable concrete strength.

5.2 Discussion

Looking at the plots on fig. 6 it is obvious that there is a trend defined as the value of the maximum compressive strength is increased. Specifically we see that the plots look virtually the same at the tension controlled regions and they diverge in the compression controlled regions as the maximum compressive strength increases. The maximum compressive strength obviously increases as the level of confinement increases. It is interesting to point out that the value of the maximum compressive strain, ε_{cu}, does not have an effect on the interactive diagram. Therefore the increase of ductility which is gained due to confinement does not play a significant role in the maximum capacity of the section. The decisive factor that affects the section capacity is the maximum compressive strength.

6 Conclusions

The following conclusions have been drawn at the end of this work:

- Confinement Increases the maximum compressive strength of the section
- Increase in the confinement reinforcement increases the capacity of the section in the compression controlled region
- Confinement affects significantly the capacity of the section when the section is in the compression controlled region (pure compression to balance point)
- The effect of confinement is small in the region between pure bending and the balance point
- Confinement has no effect in the region between pure tension and pure bending since concrete is primarily in tension. Therefore the presence of reinforcement in the hoop direction offers no improvement in concrete strength

References

[1] Michael, A. P., H. R. Hamilton III, Ansley, M. H, Concrete Confinement Using Carbon Fiber Reinforced Polymer Grid, *7th International Symposium on Fiber Reinforced Polymer (FRP) Reinforcement for Concrete Structures* (ACI 2005 Fall Convention), American Concrete Institute, Kansas City, MO, Vol. 2, pp. 991-1010, 2005.

[2] Bresler, B., Design Criteria for Reinforced Concrete Columns under Axial Load and Biaxial Bending, ACI Journal, Proceedings, Vol. 57, 1960.

[3] Parme, A. L., Nieves, J.M., Gouwens, A., Capacity of Reinforced Rectangular Columns Subjected to Biaxial Bending, ACI Journal, Proceedings, Vol. 63, No 9, 1966.

[4] Xiao, Y. and Wu, H., Compressive Behavior of Concrete Confined by Carbon Fiber Composite Jackets, *Journal of Materials in Civil Engineering*, Vol. 12, No 2, pp. 139-146, 2000.

[5] Xiao, Y. and Wu, H., A Constitutive Model for Concrete Confinement with Carbon Fiber Reinforced Plastics, *Journal of Reinforced Plastics and composites,* Vol. 22, No 13, pp. 1187-1201, 2003.

[6] Lam, L., and Teng, J. G., Ultimate Condition of Fiber Reinforced Polymer-Confined Concrete, *Journal of Composites for Construction*, Vol. 8, No 6, pp 539-548, 2004.

[7] Li, Y., Lin, C. and Sung, Y., Compressive Behavior of Concrete Confined by Various Types of FRP Composite Jackets, *Mechanics of Materials,* Vol. 35, No 3-6, pp. 603-619, 2002.

[8] Harries, K. A., and Kharel, G., Experimental Investigation of the Behavior of Variably Confined Concrete, *Cement and Concrete Research,* Vol. 33, No 6, pp. 873-880, 2002.

[9] Li, J., Hadi, M.N.S., Behaviour of Externally Confined High-Strength Concrete Columns Under Eccentric Loading, *Composite Structures*, Vol. 62, No 2, pp 145-153, 2003.
[10] Campione, G., Miraglia, N., Strength and Strain Capacities of Concrete Compression Members Reinforced with FRP, *Cement and Concrete Composites*, Vol. 25, No 1, pp 31-41, 2003.
[11] Teng, M., Sotelino, E. D., and Chen, W., Performance Evaluation of Reinforced Concrete Bridge Columns Wrapped with Fiber Reinforced Polymers, *Journal of Composites for Construction*, Vol. 7, No 2, pp 83-92, 2002.
[12] Shahawy, M, Mirmiran, A. and Beitelman, T., Tests and Modeling of Carbon-Wrapped Concrete Columns, *Composites Part B: Engineering*, Vol. 31, No 6-7, pp 471-480, 2000.
[13] Davol, A., Burgueno, R. and Seible, F., Flexural Behavior of Circular Concrete Filled FRP Shells, *Journal of Structural Engineering,* Vol. 127, No 7, pp 810-817, 2001.
[14] Park, R. and Paulay, T., Ultimate Deformation and Ductility of Members with Flexure (Chapter 6), *Reinforced Concrete Structures*, John Wiley & Sons, New York, pp 195-269, 1975.